Available online at www.sciencedirect.com
ScienceDirect
Journal of Power Sources 171 (2007) 261–267
JOURNAL OF POWER SOURCES
www.elsevier.com/locate/jpowsour

Review

Porous nickel MCFC cathode coated by potentiostatically deposited cobalt oxide III. Electrochemical behaviour in molten carbonate

M.J. Escudero [a,*], A. Ringuedé [b], M. Cassir [b], T. González-Ayuso [a], L. Daza [a,c]

[a] *Dpto. Energía, CIEMAT, Av. Complutense 22, 28040 Madrid, Spain*
[b] *Ecole Nationale Supérieure de Chimie de Paris, Laboratoire d'Electrochimie et de Chimie Analytique, UMR 7575 CNRS, 11 rue Pierre et Marie Curie, 75231 Paris Cedex 05, France*
[c] *Instituto de Catálisis y Petroleoquímica, CSIC, Campus Cantoblanco, 28049 Madrid, Spain*

Received 10 January 2007; received in revised form 4 June 2007; accepted 9 June 2007
Available online 17 June 2007

Abstract

A cobalt oxide coating was deposited on porous nickel by a potentiostatic electrochemical technique and studied in molten $(Li_{0.52}Na_{0.48})_2CO_3$ eutectics at 650 °C under an atmosphere of CO_2:Air (30:70). The structural and morphological characteristics of this coating before and after immersion in the molten electrolyte were described in a previous paper, showing that the initial Co_3O_4 layer is rapidly transformed into $LiCoO_2$ and afterwards probably into $LiCo_{1-y}Ni_yO_2$. In the present part, the electrical and electrochemical behaviour of this promising novel MCFC cathode material was thoroughly analysed during 50 h by impedance spectroscopy. A porous nickel cathode was tested in the same conditions and taken as a reference. The oxidation and lithiation reactions are accelerated by the presence of cobalt. The charge transfer resistance is higher with the coated cathode but the diffusion resistance through this new material is lower in comparison with the state-of-the-art cathode.

Keywords: Electrochemical impedance spectroscopy; Nickel oxide; Cobalt oxide; Coating; Cathode; Molten carbonate fuel cell

Contents

1. Introduction

In a previous study [1], we have investigated the behaviour of an MCFC Ni cathode, covered by electrochemically deposited cobalt oxide, in molten carbonates at 650 °C during 50 h under CO_2:Air (30:70) by XRD, Raman spectroscopy, XPS, SEM-EDS and mercury porosimetry. XRD revealed the presence of Co_3O_4 in the prepared cathode and a loss of cobalt after its immersion. Raman studies confirmed the initial presence of the Co_3O_4 spinel structure and its rapid transformation into $LiCoO_2$ and lithium–cobalt–nickel oxide ($LiCo_{1-y}Ni_yO_2$) in the molten eutectic. After exposure to the molten carbonate melt, the presence of Ni^{3+} was detected by XPS for the Co_3O_4-coated porous nickel, which is probably due to the lithiation of the NiO–Co sample. SEM micrographs revealed that the coated porous Ni

* Corresponding author. Tel.: +34 913466622; fax: +34 913466269.
E-mail address: m.escudero@ciemat.es (M.J. Escudero).

0378-7753/$ – see front matter © 2007 Elsevier B.V. All rights reserved.
doi:10.1016/j.jpowsour.2007.06.013

suffered morphologic changes during the exposure in comparison with porous Ni. This was explained by the formation of $LiCo_{1-y}Ni_yO_2$ on the surface of porous nickel. Chemical analysis confirmed the dissolution of cobalt but an important reduction in the solubility of nickel in the case of the prepared cathode. The cobalt oxide on porous nickel sample presented after its immersion similar porosity and higher pore size than the porous nickel. These results showed that this coated material presents good features in order to be used as an alternative MCFC cathode.

In the present study, the electrical characteristics of the coated material were thoroughly analysed by impedance spectroscopy in molten $(Li_{0.52}Na_{0.48})_2CO_3$ eutectics at 650 °C under a standard cathodic atmosphere of CO_2:Air (30:70). A pure porous nickel cathode was tested in the same conditions and taken as reference. This kind of analysis is of great interest in order to determine the conductivity of this cathode and to understand all the phenomena (mass and charge transfer, morphological changes, etc.) related to the electrochemical processes: these properties are essential for the selection of a good cathode material. Among the interesting studies using EIS to apprehend these phenomena, two interesting works should be mentioned. Yang and Kim [2] studied the oxidation behaviour of Ni–Co alloy deposited on a gold electrode and exposed to Li–K carbonate eutectic. They analysed the varied mechanistic processes (oxidation, diffusion, oxide growth, lithiation and oxygen reduction) by correlating OCP measurements to cyclic voltammetry and to experimental and simulated impedance data. Later, Ryu et al. [3] measured R_{ct}, R_{diff}, C_{dl} and CPE and showed their role in the understanding of the *in situ* reaction of the Ni–Co electrode, as well as the improvement of the electrocatalytic activity of Ni–Co with respect to the porous Ni cathode.

2. Experimental

2.1. Electrochemical deposition

The sample was prepared by potentiostatic deposition of cobalt oxide film on porous nickel sample according to a procedure fully described in previous papers [4,5]. The potentiostatic deposition was performed with a Princeton Applied Research (PAR) Model 263 system at 0.65 V versus SCE and an electrolysis times of 24 h. Then, the sample was annealed at 500 °C for 4 h in air at a heating rate of 1 °C min^{-1}.

2.2. Electrochemical characterisation

The electrochemical characterisation of the new cathode material was performed by means of EIS. The experimental cell used was described in previous work [6,7]. The cell was assembled with two nominally identical electrodes. Such a configuration allows elimination of the influence of the counter electrode and avoids the use of a reference electrode that is, by itself, a noise source [8]. The samples with a surface of 1 cm^2 were immersed into 75 g of lithium and sodium molten carbonates mixed in proportions of 52–48 mol% at 650 °C under a standard cathodic atmosphere of CO_2:O_2:N_2 (30:15:55). The cell impedance was measured as a function of immersion time during 50 h. A pure porous nickel cathode was tested in the same conditions and taken as reference.

The impedance spectra were recorded with an AUTOLAB with PGSTAT30 and FRA2 module (Eco Chemie B.V.). The amplitude of the sinusoidal voltage signal for the impedance measurements was 5 mV. The measurements were performed using five points per frequency decade between 100 kHz and 100 mHz at the open circuit potential. The impedance data were analysed by using the software Zview developed by J.R. McDonald.

3. Results and discussion

3.1. Previous remarks

In order to establish a sound interpretation of the impedance behaviour of Co_3O_4-coated Ni cathode, it is worthy to remind what are the important steps occurring when dipping an MCFC cathode in the molten carbonate eutectic, before reaching a stable potential due to the oxygen reduction, which can be written in a simplified mode, without taking into account O_2^{2-} or O_2^- species [9], as

$$0.5O_2 + CO_2 + 2e^- \rightarrow CO_3^{2-}$$

In the case of the nickel cathode, different steps are known to occur.

Under the cathode gaseous environment, the first step is due to nickel oxidation [10]:

$$Ni + CO_2 \rightarrow NiO + CO$$

The second step is due to the growth of the nickel oxide layer and to the increase in the resistance. Afterwards comes the third step which is the most important one for MCFC use, the influence of the alkali cations of the carbonate melt and, in particular, the lithiation phenomenon [10,11]:

$$(1-x)NiO + 0.5Li_2CO_3 + 0.25O_2 \rightarrow Li_xNi_x^{3+}Ni_{(1-2x)}^{2+}O + 0.5CO_2$$

The value of x (0.002) has been determined in a previous study [12], deducing that the lithiated compound can be represented by $Li_{0.002}Ni_{0.002}^{3+}Ni_{0.996}^{2+}O$.

The phenomenon is even more complex because, on the one hand, a slight incorporation of Na^+ is possible in the mentioned eutectic and, on the other hand, NiO can be partially dissolved in the melt [13,14]:

$$NiO + CO_2 \rightarrow Ni^{2+} + CO_3^{2-}$$

In the case of the Co_3O_4 nickel cathode, apart of the specific reaction concerning the nickel species, cobalt oxide is spontaneously transformed into $LiCoO_2$. This compound can also be slightly dissolved in the carbonate melt:

$$LiCoO_2 + 1.5CO_2 \rightarrow Li^+ + Co^{2+} + 1.5CO_3^{2-} + 0.25O_2$$

Furthermore, knowing the possible existence of the mixed $LiCo_{1-y}Ni_yO_2$ species, the phenomena involved can be rather complex.

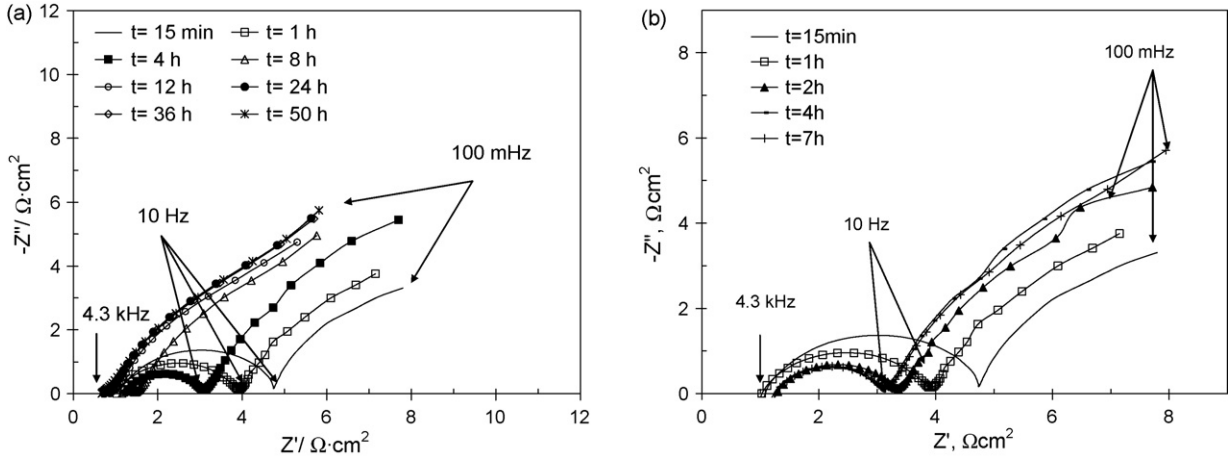

Fig. 1. Impedance diagrams of porous NiO as a function of immersion time in Li–Na eutectic, under the standard cathode gas mixture.

In brief, it is important to keep in mind all these reactions: oxidation, lithiation, dissolution, formation of mixed species, in order to have a guiding line for further interpretations.

3.2. Interpretation of impedance diagrams

Figs. 1 and 2 depict the impedance spectra as a function of the immersion time for porous NiO and porous NiO–Co, respectively, in $(Li_{0.52}Na_{0.48})_2CO_3$ at 650 °C under an atmosphere of CO_2:O_2:N_2 (30:15:55). Bode representations are shown in Figs. 3 and 4.

For the porous NiO (Fig. 1), two arcs are clearly observed during the first 8 h. Afterwards, only one semi-circular arc is perceived and its amplitude increases with the immersion time. The first arc in the high frequency region presents an important decrease when increasing the immersion time as shown in Fig. 1b, and it cannot be observed after 8 h of exposure (Fig. 1a). Bode diagrams, shown in Fig. 3, fully confirms this evolution, showing more precisely that after 12 h of immersion in the carbonate melt, both the module and the phase angle reach a stable value. The arc in the high frequency region is most probably due to charge transfer and during the first 8 h to the formation of $Li_xNi_{1-x}O$ (oxidation and lithiation). This arc tends to decrease progressively: the electrode material is stabilised and the resistance related to the physico-chemical reaction disappears; the resistance due to the charge transfer is lowered with formation of the lithiated nickel cathode. The arc in the low frequency region can be attributed to diffusion phenomena.

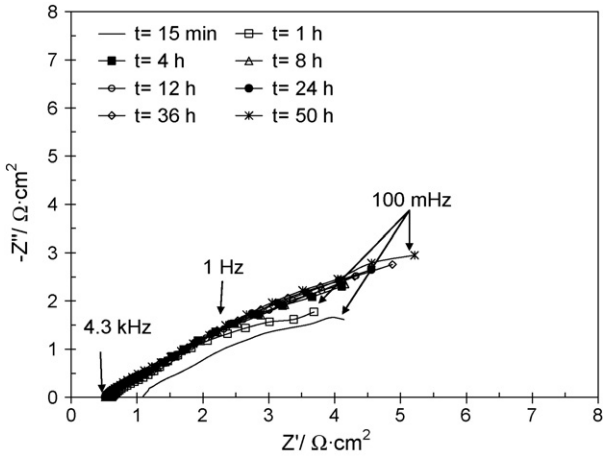

Fig. 2. Impedance diagrams of Co-coated porous NiO as a function of immersion time in Li–Na eutectic, under the standard cathode gas mixture.

In the case of the porous NiO–Co (Fig. 2), the semi-circles cannot be visually separated: it looks more like a continuous curve, mainly composed by two semi-circular arcs. The first one is small and difficult to clearly discern, whereas the second one is larger. It presents a slight enhancement during the first 4 h of exposure. After this short time, the impedance spectra do not change significantly with the exposure time. As shown in Fig. 4 (Bode diagram), a third phenomenon appears in the middle frequency range (between 5 and 100 Hz), and seems to increase with the time. As it was not confirmed by other measurements, i.e. Nyquist diagrams, it is difficult to conclude if it is an artefact or a real phenomenon.

The differences between the shape of Nyquist diagrams for the porous NiO and NiO–Co are surely due to the fact that the phenomena involved, charge transfer and diffusion, occur at significantly different frequencies for porous NiO and closer values for NiO–Co provoking an overlapping of both phenomena. This will be confirmed further on by comparing the relaxation frequencies (related to charge transfer and diffusion) corresponding to NiO and NiO–Co.

Despite the apparent difference in the shape of Nyquist diagrams for both electrode materials, the same equivalent circuit, illustrated in Fig. 5a, was used in order to compare and analyse the electrochemical behaviour of such systems. This circuit includes the self-component L, due to the electrical set-up, followed by R_e, associated to the electrolyte resistance. The interface and the electrochemical behaviour of the electrodes are represented by a typical Randles circuit, combining charge transfer process (R_{ct} and Q_{ct}) and diffusion characteristics.

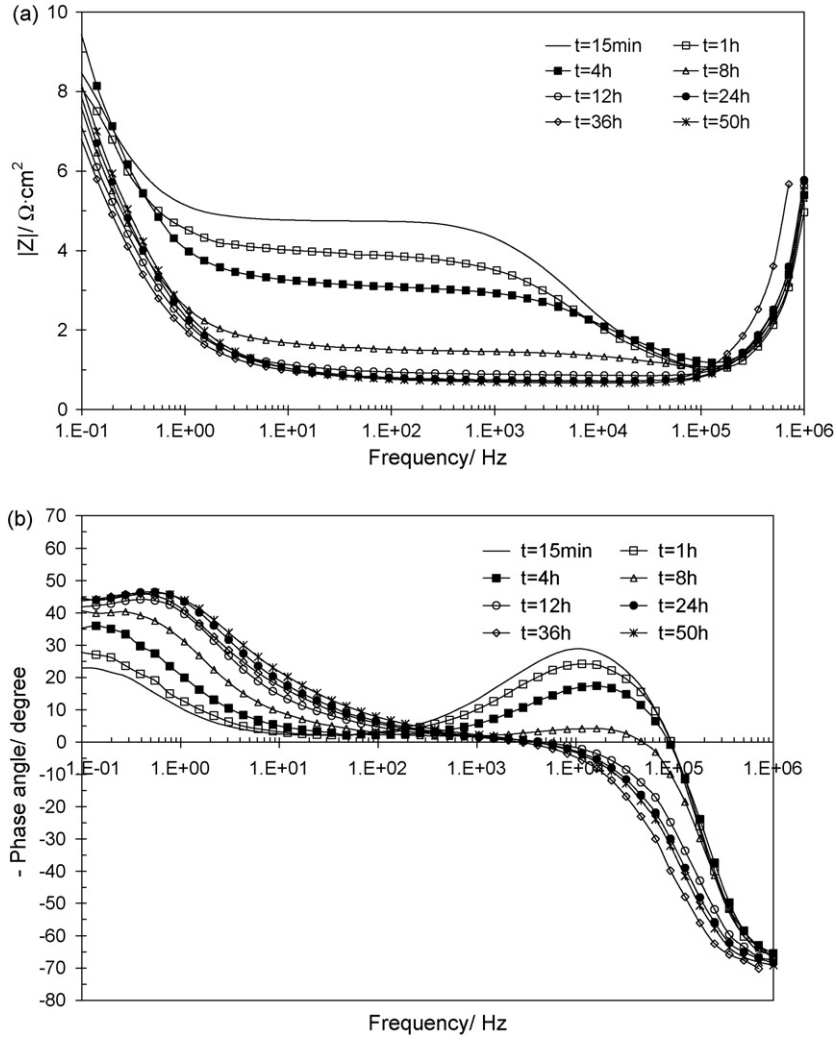

Fig. 3. Bode diagrams for NiO: (a) impedance magnitude and (b) phase angle.

Q in the equivalent circuit model represents constant phase element (CPE) taking into account that the electrode is porous and inhomogeneous. It can be defined as follows:

$$Q = \frac{1}{B(j\omega)^{\alpha}} \quad (1)$$

where B is a frequency independents constant, $\omega = 2\pi f$, j is the square root of -1, and α is an adjustable parameter, correlated to the frequency dispersion and the depressed angle of the semi-circle.

A large part of the impedance data were fitted using the general proposed equivalent circuit (Fig. 5a). In all the cases, a good agreement was found between experimental and simulated data in the whole frequency range. However, in the case of the uncoated nickel electrode, these elements were not enough to describe the whole diagram. As preliminarily announced, a first semi-circle is observed at the highest frequencies, which resistance decreases in the first 10 h. This phenomenon was represented by a typical (RQ) circuit, indexed m in Fig. 5b.

In the case of porous NiO, the oxidation and lithiation phenomena are very important until reaching a kind of equilibrium. This occurs up to 8 h approximately. The extra part of the equivalent circuit in Fig. 5b is due to the chemical (lithiation, oxidation) and physical (surface growth due to NiO formation). This phenomenon added to charge transfer resistance constitutes the first arc tending to decrease with the time. In the case of porous NiO–Co the situation is apparently simpler and no significant change is expected conducing to a simpler equivalent circuit and negligible CPE_m and and R_m.

Fig. 6 presents the evolution of the electrolyte resistance R_e, as a function of the immersion time for each tested material, i.e. porous NiO and porous NiO–Co.

As can be seen from this figure, the specific resistance measured using the porous uncoated NiO electrode, varies during the first 10 h, increasing slightly up to 1 $\Omega\,cm^2$. After 15 h of immersion, it slowly stabilises at 0.8 $\Omega\,cm^2$. The electrolyte resistance, measured using Co-coated nickel electrode, rapidly stabilises at 0.5 $\Omega\,cm^2$. As the distance between the electrodes is fixed by the experimental set-up and constant whatever the electrodes, the variations of the resistance should be only due to surface modifications. Thus, during the first 15 h, the active surface area would be higher, resulting

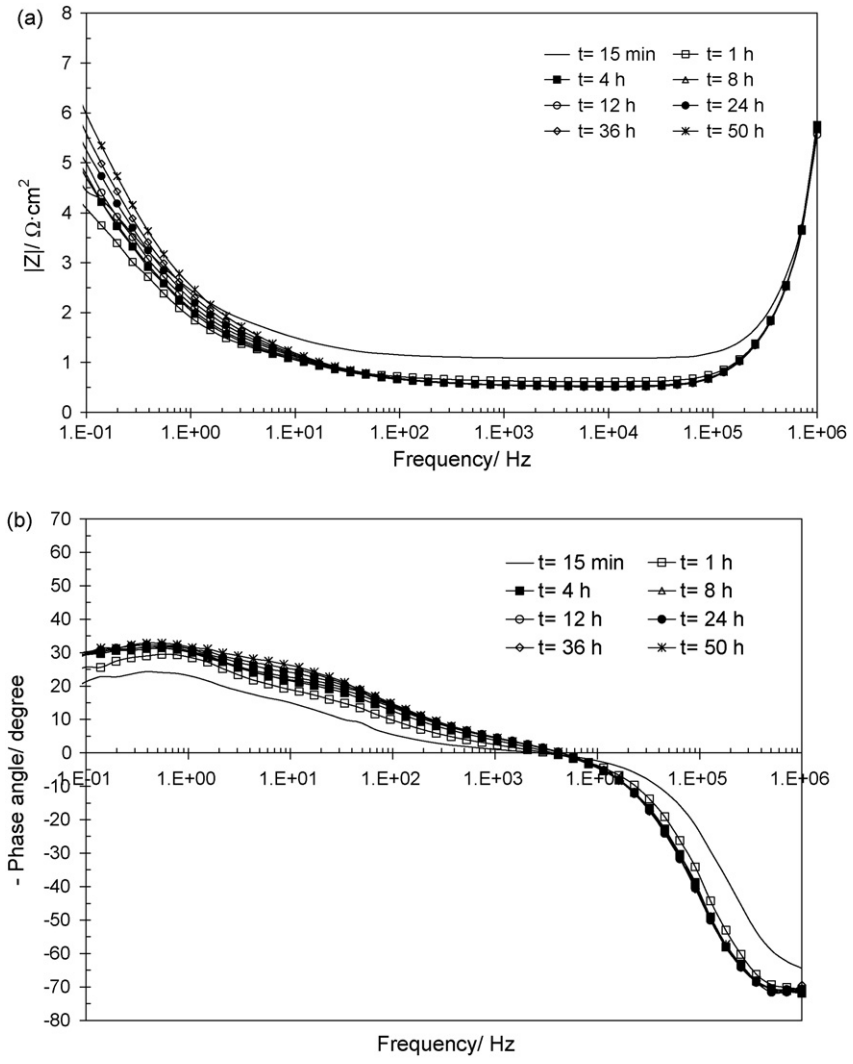

Fig. 4. Bode diagrams for NiO–Co: (a) impedance magnitude and (b) phase angle.

from the *in situ* oxidation and lithiation of the nickel electrode.

Moreover, as illustrated in Fig. 7, R_{ct} value for the porous NiO suffers an abrupt decrease during the first 12 h; beyond, its value remains constant with the immersion time, close to 0.1 $\Omega\,cm^2$. This decrease in R_{ct} values can be first explained by the change in the Ni oxidation state, from +II to +III accompanying the lithium insertion and beyond 12 h, the predominance of the electrochemical reaction resistance of oxygen reduction [2]. In the case of porous NiO–Co, a slight decrease in R_{ct} value could be observed during 0.5 h, followed by a slow continuous increase during all the immersion, reaching 2 $\Omega\,cm^2$ after 50 h. This evolution could be due to the oxidation of Ni(II) to Ni(III) and the lithiation of Ni and Co to form an oxide layer such as

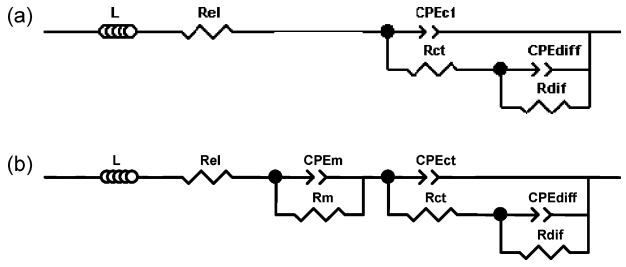

Fig. 5. Equivalent circuit used to fit: (a) the impedance diagrams; (b) the impedance diagrams, for NiO, at short times.

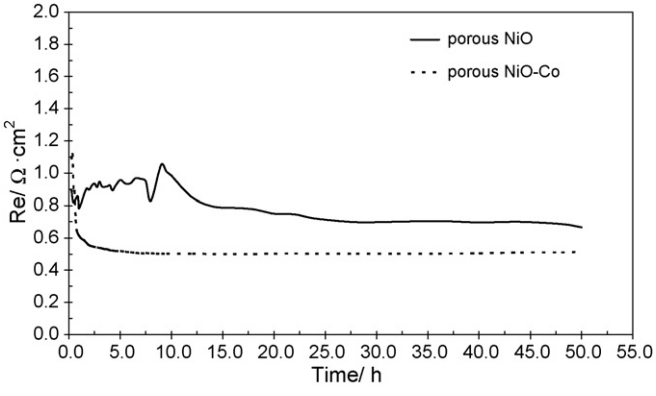

Fig. 6. Electrolyte resistance variation as a function of immersion time, for uncoated and Co-coated porous NiO.

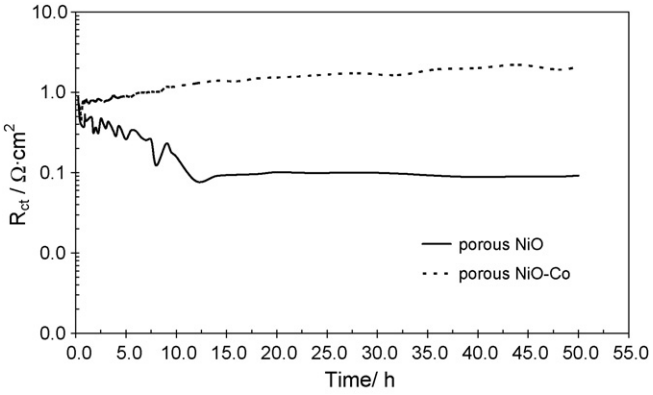

Fig. 7. Charge transfer resistance associated to NiO and NiO–Co systems, as a function of the immersion time.

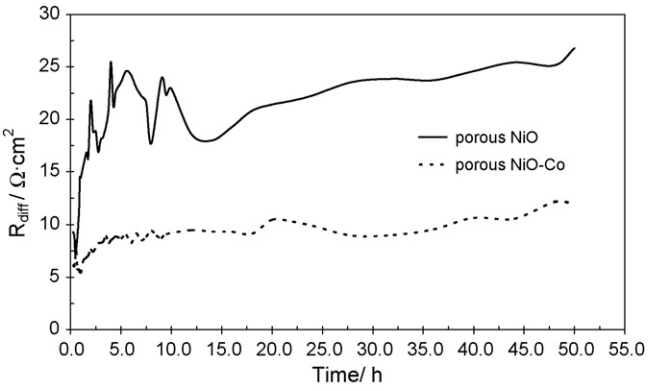

Fig. 9. Diffusion resistance for NiO and NiO–Co as a function of the immersion time.

$LiCoO_2$ and/or $LiCo_{1-y}Ni_yO_2$ on the surface of NiO. This is also combined to the resistance of the oxygen reduction reaction. Thus, fast nickel oxidation and lithiation processes occur during the first 0.5 h of exposure to the melt, after that the oxygen reduction is predominant. It shows that NiO–Co can be easily lithiated.

However, the R_{ct} is higher for the NiO–Co than for NiO, reaching a factor of 10 when both values are stabilised, indicating that the electrocatalytic activity of NiO–Co is less than that of NiO, even after lithiation and oxidation steps. There is no clear mechanistic explanation concerning the loss of electrocatalytic activity of NiO–Co with respect to NiO. $Li_xNi_{1-x}O$ is known to be a good electrocatalyst of the oxygen reduction. $LiCoO_2$ is less efficient than the state-of-the-art cathode. It seems that NiO–Co, or $LiCo_{1-y}Ni_yO_2$, has also a more moderate electrocatalytic activity. As far as we know, no clear mechanism has ever been described to explain these differences. Our results are not enough to conclude.

Fig. 8 illustrates the variation of Q_{ct} as a function of immersion time for both studied cathodes. As for the R_{ct} variations, Q_{ct} of NiO–Co presents a slight decrease during the first 0.5 h before stabilising at 6×10^{-2} F cm^{-2}, while Q_{ct} of NiO cathode varies abruptly from 100 μF cm^{-2} to 4 mF cm^{-2} after 12 h of exposure. These huge differences in the double layer capacitance values confirm that the active material is modified, not only by the phase transformation (Ni into $Li_xNi_{1-x}O$) but also in terms of surface area (the oxide surface more developed than that of the initial nickel). In the case of the Co-coated electrode, the Q_{ct} value is rapidly stabilised, confirming that the cobalt coating transformation after immersion in the carbonate melt is a quick phenomenon. The significantly higher value of Q_{ct} for the coated sample is probably due to the slower charge transfer (higher R_{ct}) and to a more developed oxide surface.

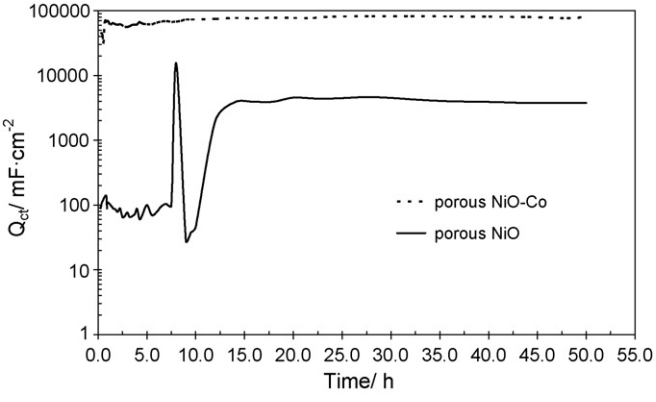

Fig. 8. Charge transfer constant phase element associated to NiO and NiO–Co systems, as a function of the immersion time.

Diffusion resistance (R_{diff}) of porous NiO and porous NiO–Co is depicted in Fig. 9. This value is about 2.5 times lower during all the immersion duration for porous NiO–Co in comparison with NiO cathode. In the case of the modified cathode, R_{diff} values are stable whatever the immersion duration. In the case of the NiO cathode, R_{diff} values are unstable during the 12 first hours, which is in agreement with the previous results showing the modification of this electrode during the lithiation–oxidation process. In effect, Li ion diffusion is predominant in the first hours, inducing the formation of a new phase at the melt/cathode interface: $Li_xNi_{1-x}O$; afterwards, the diffusion of oxide ions, such as O_2^- and O_2^{2-} becomes predominant in the electrode reaction process [2,15]. In the NiO–Co electrode, the diffusion of oxygen-reduced species seems rapidly predominant, after about 5 h. In brief, according to these experimental data, the oxygen reduction could be favoured by a more rapid diffusion towards the cathode modified with cobalt; however the reduction mechanism also depends on the charge transfer which is slower with this new electrode.

Fig. 10 shows the evolution of the relaxation frequency relative to charge transfer and diffusion for both NiO and NiO–Co cathodes. In the case of NiO, the relaxation frequency relative to the first semi-circle (short-additional phenomenon) is also determined during the first hours of immersion; the value obtained is close to that of NiO in the case of charge transfer. It is difficult at this stage to conclude precisely with respect to this phenomenon. With respect to charge transfer, it can be clearly observed that the relaxation frequency is higher in the case of NiO than of NiO–Co, which corroborates the previous results showing that charge transfer is more rapid in the case of NiO. The opposite situation is observed in the case of diffusion, which is in agreement with the fact that diffusion is faster in the case of the cobalt-modified electrode.

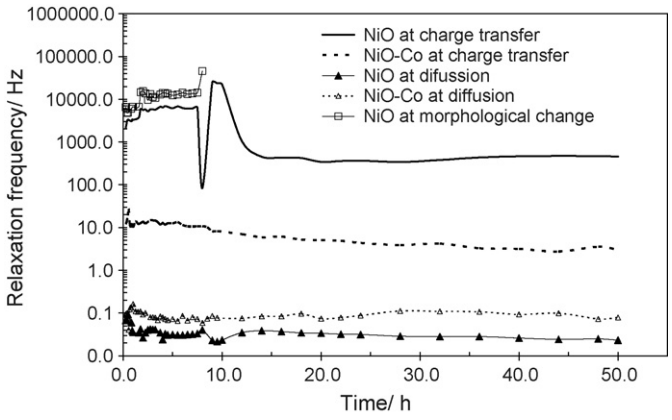

Fig. 10. Variation of relaxation frequency relative to charge transfer, diffusion for NiO and NiO–Co or NiO for short times as a function of the immersion time.

4. Conclusion

Cobalt oxide was coated on the state-of-the-art MCFC nickel cathode by an electrodeposition technique. EIS results showed two arcs, the first one at high frequency associated with the charge transfer process and the second arc in the low frequency region with a slow process (mass transfer). The impedance spectra of porous NiO presented important modifications during the first 12 h, which can be attributed to the processes of oxidation of the nickel cathode and to the incorporation of lithium in its structure. The presence of cobalt seems to accelerate the oxidation–lithiation process. The porous NiO–Co presents a higher charge transfer resistance but a lower diffusion resistance with respect to NiO. These results are in agreement with the evolution of the relaxation frequencies relative to these phenomena. Therefore, the protective coating shows an advantage (diffusion easily stabilised and more rapid) and a drawback (slower charge transfer slower) with respect to the uncoated cathode. Nevertheless, as shown in a previous paper [1], the cobalt coating decreases significantly the NiO solubility and seems to be a good alternative for a new MCFC cathode. It is difficult to give a realistic model describing the behaviour of the coated electrode, because the existence of the $Li_xNi_{1-x}O$ compound should be fully proved. All the phenomena involved are quite complex and it would be necessary to determine by other techniques (nuclear microprobe, SIMS, XPS) the concentration gradients of the species present at the surface of the electrode. Without these precious data, all the hypotheses are too speculative.

References

[1] M.J. Escudero, L. Mendoza, M. Cassir, L. Daza, J. Power Sources 160 (2006) 821.
[2] B.Y. Yang, K.Y. Kim, Electrochim. Acta 44 (1999) 2227.
[3] B.H. Ryu, S.P. Yoon, J. Han, S.W. Nam, T.-H. Lim, S.-A. Hong, K.B. Kim, Electrochim. Acta 50 (2004) 189.
[4] L. Mendoza, V. Albin, M. Cassir, A. Galtayries, J. Electroanal. Chem. 548 (2003) 95.
[5] M.J. Escudero, T. Rodrigo, L. Mendoza, M. Cassir, L. Daza, J. Power Sources 140 (2005) 81.
[6] M.J. Escudero, Ph.D. Thesis, Universidad Autónoma de Madrid, Madrid, (2002) Spain.
[7] M.J. Escudero, X.R. Nóvoa, T. Rodrigo, L. Daza, J. Appl. Electrochem. 32 (2002) 929.
[8] L. Giorgi, M. Carewska, S. Scaccia, E. Simoneti, E. Giacometti, R. Tulli, Int. J. Hydrogen Energy 21 (1996) 491.
[9] P. Tomczyck, H. Sato, K. Yamada, T. Nishina, U. Uchida, J. Electroanal. Chem. 391 (1995) 125.
[10] M.S. Yasici, J.R. Selman, Solid State Ionics 124 (1999) 1403.
[11] C. Belhomme, Ph.D. Thesis, ENSCP, University of Paris VI, 2000.
[12] C. Belhomme, M. Cassir, C. Tessier, E. Berthoumieux, Electrochem. Solid State Lett. 3 (2000) 216.
[13] M. Cassir, G. Moutiers, J. Devynck, J. Electrochem. Soc. 140 (1993) 3114.
[14] P. Tomczyk, M. Mosialek, J. Electroanal. Chem. 463 (1999) 72.
[15] M.S. Yasizi, J.R. Selman, Solid State Ionics 124 (1999) 149.